

Evaluating T-cell cross-reactivity between tumors and immune-related adverse events with TCR sequencing: pitfalls in interpretations of functional relevance

Tricia Cottrell,^{1,2,3} Jiajia Zhang,^{2,4,5} Boyang Zhang,⁶ Genevieve J Kaunitz,⁷ Poromendro Burman,^{2,4,5} Hok-Yee Chan,^{2,4,5} Franco Verde,⁸ Jody E Hooper,¹ Hans Hammers,^{4,9} Mohamad E Allaf,^{2,4} Hongkai Ji,⁶ Janis Taube,^{1,2,4,10} Kellie N Smith^{2,4,5,10}

To cite: Cottrell T, Zhang J, Zhang B, *et al.* Evaluating T-cell cross-reactivity between tumors and immune-related adverse events with TCR sequencing: pitfalls in interpretations of functional relevance. *Journal for ImmunoTherapy of Cancer* 2021;**9**:e002642. doi:10.1136/jitc-2021-002642

► Additional supplemental material is published online only. To view, please visit the journal online (<http://dx.doi.org/10.1136/jitc-2021-002642>).

TC and JZ contributed equally.

Accepted 02 June 2021

ABSTRACT

T-cell receptor sequencing (TCRseq) enables tracking of T-cell clonotypes recognizing the same antigen over time and across biological compartments. TCRseq has been used to test if cross-reactive antitumor T cells are responsible for development of immune-related adverse events (irAEs) following immune checkpoint blockade. Prior studies have interpreted T-cell clones shared among the tumor and irAE as evidence supporting this, but interpretations of these findings are challenging, given the constraints of TCRseq. Here we capitalize on a rare opportunity to understand the impact of potential confounders, such as sample size, tissue compartment, and collection batch/timepoint, on the relative proportion of shared T-cell clones between an irAE and tumor specimens. TCRseq was performed on tumor-involved and -uninvolved tissues, including an irAE, that were obtained throughout disease progression and at the time of rapid autopsy from a patient with renal cell carcinoma treated with programmed death-1 (PD-1) blockade. Our analyses show significant effects of these confounders on our ability to understand T-cell receptor overlap, and we present mitigation strategies and study design recommendations to reduce these errors. Implementation of these strategies will enable more rigorous TCRseq-based studies of immune responses in human tissues, particularly as they relate to antitumor T-cell cross-reactivity in irAEs following checkpoint blockade.

INTRODUCTION

PD(L)-1 checkpoint blockade is complicated by the development of immune-related adverse events (irAEs) in 5%–20% of treated patients.¹ Severe irAEs have been reported in up to 10% of patients and can result in hospitalization, interruption or discontinuation of therapy, and rarely, death.¹ Notably, irAEs increase in prevalence and severity with combination immunotherapy, an approach likely required to improve disappointingly low response rates.² Prediction, prevention, and treatment of irAEs will

require delineation of etiological mechanisms. One hypothesis is that irAEs are the result of cross-reactivity of an antigen-specific antitumor immune response. Supporting this hypothesis, improvements in response rates and survival in patients who develop irAEs have been observed in studies across tumor types.^{3–6} T-cell repertoire profiling with T-cell receptor sequencing (TCRseq) enables tracking of individual T-cell clones recognizing the same antigen.⁷ Multiple case series have identified shared T-cell clones in tumor and irAE tissues, thereby providing a foundation for shared antigen specificity between the tumor and irAE.^{8–10} Unfortunately, these types of analyses may be subject to several sources of confounding that are rarely considered and are often difficult to address in the context of human immune-oncology.

The current study evaluates notable sources of confounding in the analysis of T-cell receptor (TCR) repertoire overlap between tumor-involved and irAE specimens in a patient who developed a refractory irAE (dermatitis) while receiving PD-1 blockade for metastatic renal cell carcinoma (RCC). We demonstrate how these analytical pitfalls could lead to erroneous interpretation of TCRseq data obtained from distinct biological compartments and timepoints within the same patient. These factors have previously been considered as potential confounders in large-scale genomic datasets¹¹ but have not been evaluated or implemented in TCR studies.

CASE REPORT

A woman in her early 70s underwent radical nephrectomy for clear cell RCC followed by



© Author(s) (or their employer(s)) 2021. Re-use permitted under CC BY-NC. No commercial re-use. See rights and permissions. Published by BMJ.

For numbered affiliations see end of article.

Correspondence to

Dr Kellie N Smith;
ksmit22@jhmi.edu

systemic therapy, including anti-PD-1. The patient's clinical course, including development of an irAE in the form of a lichenoid dermatitis (LD),^{12–16} and biospecimen collection are shown in figure 1. The immune-related LD (irAE) persisted despite two treatment breaks and systemic prednisone (figure 1). Anti-PD-1 therapy was discontinued because of the severity of the irAE. Progressing metastases in the small bowel and a new brain metastasis were confirmed by biopsy. The patient died approximately 2 months after cessation of anti-PD-1 therapy and a rapid autopsy was performed. Findings included metastatic RCC involving the brain (specimen T_{M1}), jejunum (specimen T_{M2}), and mesentery (specimen T_{M3}). Of the three mediastinal lymph nodes (LNs) sampled, one was histologically unremarkable (LN1); one showed multiple large fibrotic nodules (LN2); and one showed multiple small subcapsular fibrotic nodules (LN3). An inflamed seborrheic keratosis (benign skin lesion) was sampled from the skin (SK) as well as uninvolved normal tissues from the left kidney and normal small bowel (NSB).

To test for possible T-cell cross-reactivity among the tumor and irAE (figure 1D), TCR V β CDR3 sequencing was performed on all specimens (online supplemental table S1).^{17 18} The irAE shared 147 unique clonotypes (4.7%) with the pretreatment primary tumor (T_p) and 118 unique clonotypes (3.7%) with jejunal metastasis (T_{M2}) (online supplemental figure S1A,B). In total, 127 unique T-cell clones present in the irAE (4.0%) were also found in at least one tumor specimen and absent in all healthy, non-lymphoid specimens (online supplemental figure S1C). We next tested if *library size* (the total number of productive sequencing reads) influences T-cell repertoire overlap among specimens. The number of clones shared with a given specimen was highly correlated with library size, illustrated for the irAE (Spearman's rho, R=0.7, p=0.031; online supplemental figure S1D, left) and LN2 (R=0.78, p=0.012; online supplemental figure S1D, right). Random subsampling weighted by clonal abundance within each specimen was used to equalize library sizes to eliminate this confounding (online supplemental figure S1E).^{7 11} Not surprisingly, a strong correlation was observed between library size and the number of unique clonotypes (R=0.93, p<2.2e⁻¹⁶; online supplemental figure S2). The degree of clonal sharing was also correlated with the number of unique clonotypes in each specimen (R=0.85 and p=0.0035 for the irAE, and R=0.92 and p=0.00047 for LN2; online supplemental figure S3A). Using weighted downsampling,^{7 11} we normalized specimens to the same library size, which eliminated the correlation between the number of unique clonotypes in a specimen and clonal sharing (online supplemental figure S3B). Therefore, we used weighted downsampling for the remainder of our analyses.

Tumor-specific T cells can be detected in paired uninvolved tissue, even when the normal tissue is collected 10–15 cm from the tumor itself.^{19–21} Likewise, clonotype sharing analyses could be confounded by bypassing viral-specific T cells. We performed a reanalysis of a

previously published functional assay^{20 21} and found that viral-specific T-cell clones showed notable clonotype sharing across multiple tissue compartments, including the tumor, in a patient with non-small cell lung cancer. A similar pattern was previously observed with neoantigen-specific T-cell clones,^{20 21} suggesting that T cells can traffic across tumor involved/uninvolved compartments regardless of the presence of antigen (online supplemental figure S4A,B). Indeed, after mapping the TCRs from our present study to a public TCR database with annotated antigen specificity (vdjdb, <https://vdjdb.cdr3.net/>), we found an Epstein-Barr Virus (EBV)-specific clone that was detected in tumor-involved tissues from our study participant (online supplemental figure S4C–D). This emphasizes that clonotype sharing alone is not necessarily associated with biological relevance. Additional abundance measurement and antigen specificity analyses are warranted to assist further interpretation. The SK and LN outliers in online supplemental figure S1D (red arrows) also indicate increased T-cell repertoire sharing between specimens from the same tissue compartment, even when collected at different locations and timepoints (ie, the irAE and SK). *Tissue compartment confounding*—a greater degree of T-cell repertoire overlap between specimens collected from the same tissue site—is illustrated with pairwise comparisons in online supplemental figure S5A,B. While T-cell repertoire sharing is reduced in samples from different tissue compartments, shared clones are still detected between seemingly unrelated specimens. These could reflect circulating clones at the time of tissue collection and are not necessarily reflective of biologically meaningful clonal sharing, (ie, *batch effect confounding*). We used the Morisita Overlap Index (MI), which incorporates relative clonal abundance and is not influenced by library size in our dataset (online supplemental figure S6A), to calculate the overlap between the irAE and all other specimens. The relative clonal sharing among all specimens is illustrated in a chord diagram (online supplemental figure S6B), in which the width of the bands is proportional to the MI values. The highest MI was observed between specimens collected from the same batch and from the same tissue compartment (online supplemental figure S6C). These population-level comparisons likely capture a combination of biological and batch effects, which cannot be distinguished in this dataset.

We next tested for evidence of cross-reactive T cells in the tumor and irAE while accounting for the sources of confounding identified previously (figure 1E). Within the limitations of specimen availability, tissue compartment and batch effect were considered in selecting comparator specimens for meaningful analyses. First, the T-cell repertoire overlap between the primary tumor and the metastases was quantified using MI, which demonstrated a significantly higher overlap among the progressing metastases relative to the mediastinal LNs and normal tissues (p=0.044; figure 1F,G). A chord diagram highlights population-level sharing among all tumor specimens

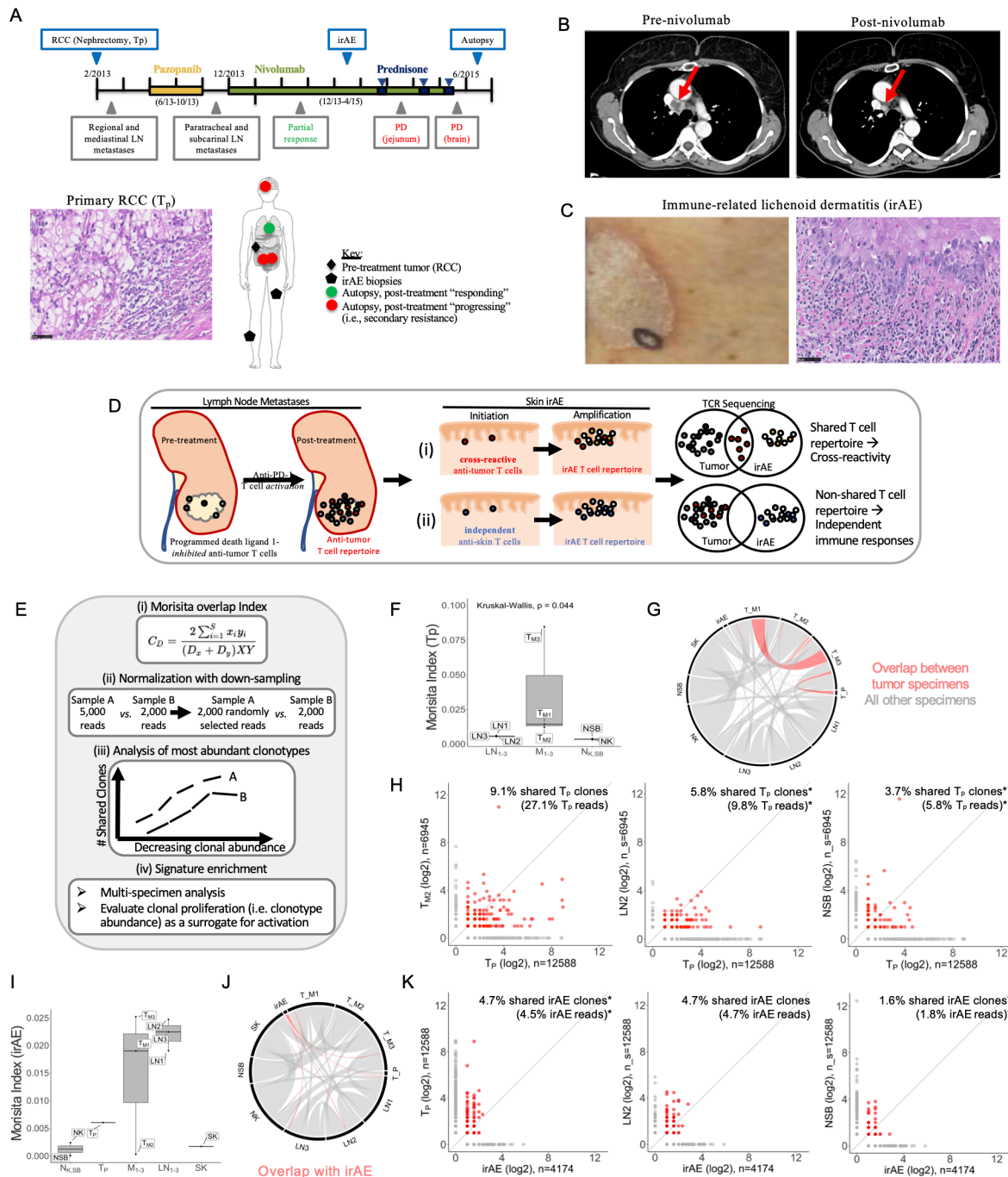


Figure 1 Clinical course and assessment of TCR repertoire overlap among tumor specimens and the irAE. (A) Timeline shows the clinical course from RCC resection to autopsy. Therapies included pazopanib (yellow bar), nivolumab (green bar), and prednisone (blue bars), with treatment dates shown below the bars. Radiographical assessments (gray boxes) included mediastinal metastases with partial response to nivolumab followed by PD in the bowel and brain. Tissue specimens collected (blue boxes) included the resected RCC (photomicrograph shown), biopsies of the immune-related lichenoid dermatitis (irAE), and multiple specimens collected at the time of rapid autopsy (see online supplemental table S1). The anatomical sites of the collected specimens are illustrated, including the primary renal tumor (black diamond), two sites of irAE (black pentagons), mediastinal LNs at the site of tumor regression (green circles) and progressing lesions in the jejunum, mesentery, and brain (red circles). (B) Intravenous contrast-enhanced CT of the chest demonstrated right lower paratracheal adenopathy which resolves after nivolumab treatment (red arrow). (C) A photograph (left) and photomicrograph (right) of the irAE, the latter showing the brisk lichenoid lymphocytic infiltrate and necrotic keratinocytes. (D) Diagram illustrating two hypotheses for the development of irAEs following immune checkpoint blockade: (i) the cross-reactivity hypothesis proposed that T cells activated as part of the antitumor immune response cross-react at the site of the irAE; this would be supported by detection of overlapping TCR repertoire signatures between the tumor and irAE; in contrast, if the irAE and antitumor immune responses were independent of each other, it was unlikely significant TCR repertoire overlap between the two sites would be detected. All photomicrographs

Figure 1 (Continued)

at $\times 400$ magnification, scale bars 50 μm . (E) Proposed approaches to maximize interpretive value and minimize confounding in TCR sequencing data analysis, including (i) the MI for quantifying global TCR repertoire sharing among multiple specimens in a sample size-independent manner, (ii) proportional downsampling for library size normalization to enable relative interpretations of clonal sharing, and (iii) normalization to relative clonal abundance in each specimen to assess relative sharing among the most abundant T-cell clones across multiple specimens. (F) The Morita index demonstrates that the three metastatic lesions consistently showed a greater degree of sharing with the T_p (MI median 0.014, range 0.012–0.088) relative to the normal control tissues (NSB MI 0.004, NK MI 0.003). (G) Chord diagram illustrates TCR repertoire overlap among the T_p and multiple post-treatment progressing metastases (red). Non-tumor specimens are shown in gray. (H) Following library size normalization, a metastasis (TM2, left), LN (LN2, middle), and NSB (right) were evaluated for T-cell repertoire overlap with the primary tumor (TP). Clonal expansion of clones shared with TM2 is suggested by 9.1% of shared TP clonotypes representing 27.1% of TP reads. Subsampled comparisons are indicated (*) and the 95% CIs for shared TP clones were 5.2% to 6.8% for LN2 (middle, representing 4.9%–15.8% total TP reads) and 3.3% to 4.3% for NSB (right, representing 3.5%–14.7% total TP reads). (I) The Morita Index demonstrates an overall low degree of TCR repertoire between the irAE and the other specimens, although the relative sharing with two of the three metastatic lesions (MI median 0.02, range 0.0003–0.026) and the three regression site LNs (MI median 0.025, range 0.021–0.027) was higher than with the normal tissues (NSB MI 0.00004, NK MI 0.003). (J) Chord diagram highlighting sharing with the irAE as assessed by the MI in red (sharing among other specimens shown in gray for reference). (K) Following library size normalization, pairwise quantification of shared clones shows that while 4.7% of irAE clones were shared with the primary tumor and a regression site LN (LN2, 95% CI 4.6% to 5.9% irAE clones), the shared clones were not expanded in the irAE (representing 4.5% and 4.7%, 95% CI 4.7% to 6.4% of the total irAE reads, respectively). Sharing between the irAE and NSB shown for comparison, 1.6% shared clones (95% CI 1.3% to 2.2%) represent 1.8% total irAE reads (95% CI 1.3% to 2.2%). Subsampled comparisons are indicated (*). (L) The GLIPH2 clustering algorithm was used to detect and quantify potential specificity clusters based on TCR CDR3 sequencing information. Motif clusters were included in downstream analysis if there were ≥ 3 unique CDR3s, ≥ 10 reads for each CDR3, a vb score < 0.05 , and a length score of < 0.05 . The barplot shows the clonal abundance of the significantly enriched ‘SSQD’ motif in the dermatitis and respective clonal abundance in other tissue compartments. GLIPH2, grouping lymphocyte interactions by paratope hotspots 2; irAE, immune-related adverse event; LN, lymph node; MI, Morisita Overlap Index; NK, normal tissues from the left kidney; NSB, normal small bowel; PD, progressive disease; RCC, renal cell carcinoma; SK, skin; TCR, T-cell receptor; T_p , pretreatment primary tumor.

(figure 1G), with the greatest TCR repertoire overlap observed between the metastases from the brain (T_{M1}) and mesentery (T_{M3} , MI 0.47). Although batch effect is a potential confounder, this degree of overlap is not observed with the small bowel metastasis (T_{M2} , MI 0.03 and 0.04 with T_{M1} and T_{M3} , respectively), also collected at autopsy. Since the primary tumor and metastases were collected at different time points and from different tissue sites, batch and tissue compartment effects could not be confounders in this analysis. We recognize that a small sample size limits interpretation of the aforementioned findings, given that T_{M1} and T_{M3} have the smallest library sizes (online supplemental table S1), even though they satisfied our criteria for inclusion. Consequently, we focused on the metastasis with the largest library size (T_{M2} , 6945 reads) for additional analyses.

Following library size normalization, 9.1% of unique primary tumor clonotypes are shared with T_{M2} relative to 5.8% (95% CI 5.2% to 6.8%) and 3.7% (95% CI 3.3% to 4.3%) of T_p clonotypes shared with LN2 and NSB, respectively (figure 1H). Clonal expansion of shared clones in the primary tumor was greatest for those shared with T_{M2} , with shared clones representing 27.1% of total primary tumor reads. The TCR repertoire overlap between the primary tumor and LN2 may suggest an antitumor signature in the mediastinal LNs, a site of radiographical tumor regression. The same approach was used to evaluate TCR repertoire overlap between the irAE and tumor specimens. The irAE repertoire was most similar to T_{M3} , T_{M1} , and the regression site LNs (figure 1I), with intermediate overlap with T_p and the least overlap with the normal control specimens. Although the relative degrees

of overlap with the irAE potentially suggest a biologically relevant pattern, the magnitude of population-level TCR repertoire sharing is quite small relative to values observed among other specimens (figure 1J).

Specimen libraries were then normalized to allow direct pairwise comparison of clonal sharing with the irAE. Sharing between the irAE and T_p (largest library size of 12,588 reads) was compared with LN2 and NSB. A similar degree of irAE clonotype sharing was observed in T_p and LN2, which was greater than that observed for NSB (figure 1K). There was no evidence of clonal proliferation in the irAE or T_p (figure 1K). Finally, we evaluated the most abundant clonotypes in each specimen for overlap with the irAE, given that prior studies have implicated the highest-frequency intratumor clonotypes in mediating antitumor immunity.²² There was no enrichment of irAE-shared clones in the tumor relative to the non-tumor specimens (online supplemental figure S7).

Based on observations that antigen specificity may be determined by limited contact sites in the TCR CDR3, we applied the grouping lymphocyte interactions by paratope hotspots 2 (GLIPH2) algorithm^{23 24} to identify and cluster TCR sequences into possible antigen specificity groups. In order to be included in downstream analyses, clusters had to contain ≥ 3 unique CDR3s, ≥ 10 reads for each CDR3, a variable gene beta (vb) score of < 0.05 , and a length score < 0.05 . One cluster with significant enrichment in the irAE was identified. Notably, the primary tumor (3.66%) had the highest abundance of T-cell clones in the ‘SSQD’ CDR3 motif cluster (figure 1L), followed by the irAE (2.42%), which were both higher than representation of this motif in non-diseased TCR repertoires

from four healthy donors (range: 0.03%–1.67%, online supplemental figure S8).²⁵ Though the human leukocyte antigen (HLA) information is unknown, three of the four healthy donors had common clonotypes shared with the patient in our study, indicating that at least one HLA allele was shared among them. By querying additional published skin/tumor-reactive TCR data, the specific motif SSQD was reported in a T-cell clone recognizing an epitope derived from Maspin, which functions as a tumor suppressor gene in epithelial cells.²⁶ Collectively, this indicates that, though analyses of the total TCR repertoire and a subset of high abundance clones do not show a signature of enriched sharing between the irAE and tumor specimens relative to non-tumor specimens at the clonotype level, more ‘antigen-driven’ approaches may be useful to identify potential specificity clusters, especially when coupled with functional assays to confirm antigen specificity and cross-reactivity between irAEs and tumors.

DISCUSSION

As immune checkpoint blocking agents become first-line and second-line therapies for a growing number of tumor types, we are faced with an increasing number of diverse irAEs that may develop during or after treatment. The association of cutaneous irAEs with clinical benefit in some patients suggests that there may be a common antigen that may underlie both durable antitumor responses and clinically significant irAEs. It is conceivable that T cells with a common TCR could mediate both tumor regression and irAE development and progression, as has been evidenced by prior studies evaluating clonal overlap of TCR clonotypes between tumor and irAE tissues^{8–10} and that expansion of peripheral blood T-cell clones prior to irAE onset positively correlates with irAE severity during checkpoint blockade treatment.²⁷

The large number and circulating nature of T cells predispose these studies to detecting false positive signals, that is, detection of differential or statistically significant clonal overlap that is not necessarily of pathogenic relevance. Biological differences exacerbate this issue, including variation in T-cell numbers and clonality in different tissue types. In addition, due to differences in sampling, clonotype detection can be limited, particularly for rare/low-frequency clonotypes. The analysis pitfalls and mitigation strategies identified in this study are summarized in [table 1](#), and we present considerations for prospective specimen collection in online supplemental figure S9. Many of these factors are already considered as a standard part of large-scale genomic analyses, but they are not yet routinely applied to immune receptor sequencing datasets and, to date, no studies have demonstrated the differential outcomes when these important sources of confounding are not acknowledged. Strengths of this study include the rare opportunity to analyze the TCR repertoire in the same patient across time, tissue compartments, and disease states, and the ability to compare with published tumor-reactive/skin-reactive

TCRs and non-irAE skin TCRs. We recognize that we are limited in our ability to comprehensively dissect all potential sources of confounding owing to limited sample availability. Lastly, the data-driven recommendations made in this study highlight the scientific value of rapid autopsy to answer complex questions using human tissue specimens.

METHODS

Case selection

Specimens from the underlying primary tumor and/or metastatic site and from skin affected by the cutaneous irAE were collected from the Johns Hopkins Hospital surgical pathology archives and the Rapid Autopsy program and Franklin Square Hospital. Overall patient response to anti-PD-1 therapy was classified according to Response Evaluation Criteria in Solid Tumors V.1.1.

TCRseq and bioinformatic analysis

DNA extraction from formalin-fixed paraffin-embedded (FFPE)-preserved tumor and skin biopsy specimens was performed using the DNeasy Blood and Tissue Kit (Qiagen). The TCR-B locus was amplified and sequenced using the ImmunoSEQ assay (Adaptive Biotechnologies). Non-productive TCR CDR3 sequences (premature stop or frameshift), sequences with amino acid length less than 7, and sequences not starting with ‘C’ or ending with ‘F/W’ were excluded from the final analyses. Specimens with at least 1000 reads were included in the final analysis. To focus on T cells recognizing the same antigen, we analyzed amino acid clonotypes exclusively.

The degree of clonality for each specimen was assessed by the productive clonality matrix, which is defined as 1-Pielou’s evenness.²⁸ Values near one represent samples with one or a few predominant clones (monoclonal or oligoclonal samples), whereas values near 0 represent a polyclonal population.

A random subsampling approach weighted by clonal abundance was used to equalize library sizes for relative comparisons of TCR repertoire overlap. For subsampling, each clonotype at amino acid level was treated as a sample and specimens were randomly sampled with replacement and weighted by clonal abundance (or frequency) until the total read count equaled that of the comparator library. To account for subsampling variation, the procedure was repeated 100 times and the 95% CIs for all subsampled comparisons are reported.

The degree of T cell clone overlap at the species level was evaluated using the Morisita overlap index.^{29 30} This measurement accounts for differences in library size and diversity per specimen, values near one the species occur in the same proportion in both samples, whereas values near 0 implies the two samples do not overlap in terms of species. Clonotypic sharing at the individual clone level was assessed in pairwise biological compartments before and after normalization to the same library size. Clones that were copresented in any of the compartment pairs are defined as shared clones. Based on the clonal frequency

**Table 1** Mitigating pitfalls and approaches for interpretation of TCRseq data

Potential confounders	Pitfall	Mitigation
Batch effect	Circulating T-cell clones may be 'shared' by multiple specimens collected at the same time point.	Control normal tissue(s) collected at the same timepoint can be used to identify these background clones.
Blood	During active immune responses,* both relevant and non-relevant clones circulate in blood.	Functional assays enable identification of disease-relevant clones (vs batch background).
Tissue compartment effect	Specimens from the same organ share tissue resident T cells, including antitumor clones. ¹⁹	Clonotype sharing with 'paired' normal tissue does not preclude biological relevance. Measurements such as abundance and antigen specificity (antigen-driven clustering/functional assays) are needed for further discernment.
Library size variation	Increased read count→more clones sampled→a larger proportion of shared clones	Analyses must correct for sample size variation (eg, Morisita Overlap Index, normalization, etc)
LN/lymphoid-rich tissues	Increased probability of repertoire overlap given large, diverse T-cell populations	Avoid analysis of background lymphoid tissue in LN metastases; interpret LN data with caution.
Interpretation	Definition	Approach
Clonal abundance (relative read count)	Relative proportion of sequencing reads for a unique clonotype (surrogate for clonal proliferation)	Assess for signals of clonal proliferation in relevant tissues to suggest functional relevance.†
Low abundance	Meaningful threshold for exclusion of 'background' clones has not been rigorously defined	Exclude specimens with <1000 reads. Sample size informs interpretation of low-read clones.
High abundance	Increasing abundance suggests clonal proliferation (and antigen exposure) in a given tissue.*	Proliferation of shared clones in disease-relevant tissues supports potential mechanistic overlap.
TCR repertoire sharing	Mechanistic interpretations of TCR repertoire overlap are limited by several confounders.	Multispecimen analyses, antigen-driven clustering (such as GLIPH2), and functional assays maximize interpretability of TCRseq data.

*During tumor killing (early in treatment) or active autoimmunity (immune-related adverse events).

†Assuming systemic clonal proliferation (batch effect) has been excluded.

GLIPH2, grouping lymphocyte interactions by paratope hotspots 2; LN, lymph node; TCR, T-cell receptor; TCRseq, T-cell receptor sequencing.

distributions (online supplemental figure 4), we assessed the top 40 clones in each specimen for overlap with the irAE repertoire. GLIPH2^{23 24} was used for antigen-specific clustering. The motif significantly-enriched in the irAE was queried in a published dataset of tumor-reactive/skin-reactive TCRs in lung cancer²⁶ and in a dataset of dermal/epidermal TCRs from healthy donors.²⁵

Statistical analysis

Statistical analysis was performed using R software. The Mann Whitney U test was used for comparison of 2-group data. For analysis of >2 group data, Kruskal-Wallis was used. Spearman's rho correlation was used to determine correlation significance. TCR preprocessing was performed using tcR package. Chord diagram was performed using the circlize package.^{31 32} $p < 0.05$ was considered significant.

Data and code availability

Bulk TCR V β sequencing data generated by Adaptive Biotechnologies are available in the Adaptive

Biotechnologies ImmuneACCESS repository at DOI: 10.21417/TRCJZ2021JITC. The code to perform down-sampling of the TCR repertoire to the same library size and relevant figures are available online (<https://github.com/BKI-immuno/dermatitis/>).

Author affiliations

¹Department of Pathology, Johns Hopkins University School of Medicine, Baltimore, Maryland, USA

²Bloomberg-Kimmel Institute for Cancer Immunotherapy, Baltimore, MD, USA

³Queen's Cancer Research Institute at Queens University, Kingston, Ontario, Canada

⁴Sidney Kimmel Comprehensive Cancer Center, Baltimore, Maryland, USA

⁵Department of Oncology, Johns Hopkins University School of Medicine, Baltimore, MD, USA

⁶Department of Biostatistics, Johns Hopkins University, Baltimore, Maryland, USA

⁷Department of Dermatology, Johns Hopkins University School of Medicine, Baltimore, Maryland, USA

⁸Department of Radiology, Johns Hopkins School of Medicine, Baltimore, MD, USA

⁹Harold C. Simmons Comprehensive Cancer Center, Dallas, TX, USA

¹⁰The Mark Foundation Center for Advanced Genomics and Imaging, Baltimore, MD, USA

Twitter Hongkai Ji @jihk99 and Kellie N Smith @SmithImmunology

Acknowledgements We thank the patient and the patient's family for participation in this study, members of our research and administrative teams who contributed to this study, and also Fiamma Berner and Lukas Platz for generous and prompt tumor-reactive/skin-reactive T-cell receptor sequencing data sharing.

Contributors TC, GJK, and H-YC conceived of and conducted the experiments. KNS and JT oversaw the study design, data interpretation, and manuscript preparation. JZ, BZ, PB, and HJ led the bioinformatic analyses. FV, JEH, HH, and MEA oversaw the clinical care of the patient and led the specimen acquisition. All authors contributed to and edited the manuscript.

Funding KNS was supported by the Lung Cancer Foundation of America, the IASLC Foundation, Swim Across America, and The Commonwealth Foundation. KNS, JT, JZ, and BZ were supported by the Mark Foundation for Cancer Research. HJ was partially supported by the National Institutes of Health (NIH)/National Human Genome Research Institute (grant R01HG009518). TC was supported by NIH (T32 CA193145). KNS and HJ were supported by R37 CA251447. This research was funded in part through the Bloomberg-Kimmel Institute for Cancer Immunotherapy, Bloomberg Philanthropies, and P30CA006973.

Competing interests HH has received clinical research funding from Bristol-Myers Squibb and Merck and serves in an advisory role for Pfizer, Merck, and Bristol-Myers Squibb. JT receives research funding from Bristol-Myers Squibb and serves a consulting/advisory role for Bristol-Myers Squibb, Merck, and Astra Zeneca. KNS has received travel support/honoraria from Illumina, Inc., receives research funding from Bristol-Myers Squibb, Enara Bio, and Astra Zeneca, and owns founder's equity in manaT Bio. The terms of all these arrangements are being managed by the investigators' respective institutions in accordance with their conflict of interest policies.

Patient consent for publication Not required.

Ethics approval This study was approved by the institutional review board (IRB) at Johns Hopkins University (JHU) and was conducted in accordance with the Declaration of Helsinki and the International Conference on Harmonization Good Clinical Practice guidelines. The patient described in this study provided written informed consent as approved by the IRB of JHU.

Provenance and peer review Not commissioned; externally peer reviewed.

Supplemental material This content has been supplied by the author(s). It has not been vetted by BMJ Publishing Group Limited (BMJ) and may not have been peer-reviewed. Any opinions or recommendations discussed are solely those of the author(s) and are not endorsed by BMJ. BMJ disclaims all liability and responsibility arising from any reliance placed on the content. Where the content includes any translated material, BMJ does not warrant the accuracy and reliability of the translations (including but not limited to local regulations, clinical guidelines, terminology, drug names and drug dosages), and is not responsible for any error and/or omissions arising from translation and adaptation or otherwise.

Open access This is an open access article distributed in accordance with the Creative Commons Attribution Non Commercial (CC BY-NC 4.0) license, which permits others to distribute, remix, adapt, build upon this work non-commercially, and license their derivative works on different terms, provided the original work is properly cited, appropriate credit is given, any changes made indicated, and the use is non-commercial. See <http://creativecommons.org/licenses/by-nc/4.0/>.

REFERENCES

- Martins F, Sofiya L, Sykiotis GP, *et al*. Adverse effects of immune-checkpoint inhibitors: epidemiology, management and surveillance. *Nat Rev Clin Oncol* 2019;16:563–80.
- Haslam A, Prasad V. Estimation of the percentage of US patients with cancer who are eligible for and respond to checkpoint inhibitor immunotherapy drugs. *JAMA Netw Open* 2019;2:e192535.
- Weber JS, Kähler KC, Hauschild A. Management of immune-related adverse events and kinetics of response with ipilimumab. *J Clin Oncol* 2012;30:2691–7.
- Freeman-Keller M, Kim Y, Cronin H, *et al*. Nivolumab in resected and unresectable metastatic melanoma: characteristics of immune-related adverse events and association with outcomes. *Clin Cancer Res* 2016;22:886–94.
- Das S, Johnson DB. Immune-Related adverse events and anti-tumor efficacy of immune checkpoint inhibitors. *J Immunother Cancer* 2019;7:306.
- Xing P, Zhang F, Wang G, *et al*. Incidence rates of immune-related adverse events and their correlation with response in advanced solid tumors treated with NIVO or NIVO+IPI: a systematic review and meta-analysis. *J Immunother Cancer* 2019;7.
- Rosati E, Dowds CM, Liaskou E, *et al*. Overview of methodologies for T-cell receptor repertoire analysis. *BMC Biotechnol* 2017;17:61.
- Läubli H, Koelzer VH, Matter MS, *et al*. The T cell repertoire in tumors overlaps with pulmonary inflammatory lesions in patients treated with checkpoint inhibitors. *Oncoimmunology* 2018;7:e1386362.
- Johnson DB, Balko JM, Compton ML, *et al*. Fulminant myocarditis with combination immune checkpoint blockade. *N Engl J Med* 2016;375:1749–55.
- Berner F, Bomze D, Diem S, *et al*. Association of checkpoint inhibitor-Induced toxic effects with shared cancer and tissue antigens in Non-Small cell lung cancer. *JAMA Oncol* 2019;5:1043.
- Zhang J, Ji Z, Smith KN. Analysis of TCR β CDR3 sequencing data for tracking anti-tumor immunity. *Methods Enzymol* 2019;629:443–64.
- Chou S, Hwang SJE, Carlos G, *et al*. Histologic assessment of lichenoid dermatitis observed in patients with advanced malignancies on Antiprogramed cell death-1 (anti-PD-1) therapy with or without ipilimumab. *Am J Dermatopathol* 2017;39:23–7.
- Curry JL, Tetzlaff MT, Nagarajan P, *et al*. Diverse types of dermatologic toxicities from immune checkpoint blockade therapy. *J Cutan Pathol* 2017;44:158–76.
- Hwang SJE, Carlos G, Wakade D, *et al*. Cutaneous adverse events (AEs) of anti-programmed cell death (PD)-1 therapy in patients with metastatic melanoma: A single-institution cohort. *J Am Acad Dermatol* 2016;74:455–61.
- Schaberg KB, Novoa RA, Wakelee HA, *et al*. Immunohistochemical analysis of lichenoid reactions in patients treated with anti-PD-L1 and anti-PD-1 therapy. *J Cutan Pathol* 2016;43:339–46.
- Tetzlaff MT, Nagarajan P, Chon S, *et al*. Lichenoid dermatologic toxicity from immune checkpoint blockade therapy: a detailed examination of the clinicopathologic features. *Am J Dermatopathol* 2017;39:121–9.
- Robins HS, Campregher PV, Srivastava SK, *et al*. Comprehensive assessment of T-cell receptor beta-chain diversity in alphabeta T cells. *Blood* 2009;114:4099–107.
- Carlson CS, Emerson RO, Sherwood AM, *et al*. Using synthetic templates to design an unbiased multiplex PCR assay. *Nat Commun* 2013;4:2680.
- Zhang J, Ji Z, Caushi JX, *et al*. Compartmental analysis of T-cell clonal dynamics as a function of pathologic response to neoadjuvant PD-1 blockade in resectable non-small cell lung cancer. *Clin Cancer Res* 2020;26:1327–37.
- Daniilova L, Anagnostou V, Caushi JX, *et al*. The mutation-associated neoantigen functional expansion of specific T cells (MANAFEST) assay: a sensitive platform for monitoring antitumor immunity. *Cancer Immunol Res* 2018;6:888–99.
- Forde PM, Chaft JE, Smith KN, *et al*. Neoadjuvant PD-1 blockade in resectable lung cancer. *N Engl J Med* 2018;378:1976–86.
- Zhang J, Ji Z, Caushi JX, *et al*. Compartmental analysis of T-cell clonal dynamics as a function of pathologic response to neoadjuvant PD-1 blockade in resectable non-small cell lung cancer. *Clin Cancer Res* 2019.
- Huang H, Wang C, Rubelt F, *et al*. Analyzing the Mycobacterium tuberculosis immune response by T-cell receptor clustering with GLIPH2 and genome-wide antigen screening. *Nat Biotechnol* 2020;38:1194–202.
- Glanville J, Huang H, Nau A, *et al*. Identifying specificity groups in the T cell receptor repertoire. *Nature* 2017;547:94–8.
- Cheuk S, Schlums H, Gallais Sérézal I, *et al*. CD49a expression defines tissue-resident CD8⁺ T cells poised for cytotoxic function in human skin. *Immunity* 2017;46:287–300.
- Berner F, Bomze D, Diem S, *et al*. Association of checkpoint inhibitor-induced toxic effects with shared cancer and tissue antigens in non-small cell lung cancer. *JAMA Oncol* 2019;5:1043–7.
- Subudhi SK, Aparicio A, Gao J, *et al*. Clonal expansion of CD8 T cells in the systemic circulation precedes development of ipilimumab-induced toxicities. *Proc Natl Acad Sci U S A* 2016;113:1919–24.
- Kirsch I, Vignali M, Robins H. T-cell receptor profiling in cancer. *Mol Oncol* 2015;9:2063–70.
- Wolda H. Similarity indices, sample size and diversity. *Oecologia* 1981;50:296–302.
- Morisita M. Measuring of the dispersion and analysis of distribution patterns. In: *Memoires of the faculty of science*. Kyushu University, 1959.
- Gu Z, Gu L, Eils R, *et al*. circlize implements and enhances circular visualization in R. *Bioinformatics* 2014;30:2811–2.
- Nazarov VI, Pogorelyy MV, Komech EA, *et al*. tCR: an R package for T cell receptor repertoire advanced data analysis. *BMC Bioinformatics* 2015;16:175.